LI-RADS for Diagnosing Hepatocellular Carcinoma in Patients with Noncirrhotic Chronic Hepatitis C

Jihyun An, MD, PhD*1 • Rohee Park, MD*2 • Euichang Kim, MD3 • Seong Kyun Na MD, PhD4,5 • Ha Il Kim, MD, PhD1 • In-Hye Song, MD, PhD6,7 • Young Seo Cho, MD, PhD8 • Ji Hun Kang, MD, PhD8 • Han Chu Lee, MD, PhD1,7 • Seungbong Han, PhD9 • Jean-Charles Nault, MD, PhD10,11,12 • Sang Hyun Choi, MD, PhD**2,7 • Ju Hyun Shim, MD, PhD**3,7

* J.A. and R.P. contributed equally to this work.

** S.H.C. and J.H.S. are co–senior authors.

Author affiliations, funding, and conflicts of interest are listed at the end of this article.

See also the editorial by Schöllnast in this issue.

Background: The Liver Imaging Reporting and Data System (LI-RADS) criteria have not been validated for patients with noncirrhotic chronic hepatitis C (CHC), who are at a greater risk for hepatocellular carcinoma (HCC) than the general population.

Purpose: To evaluate the diagnostic performance of LI-RADS category 5 (LR-5, indicating definite HCC) observations for HCC using CT and MRI in patients with noncirrhotic CHC and to compare these findings with those in patients with cirrhotic CHC.

Materials and Methods: This retrospective study included patients without cirrhosis with CHC with focal hepatic nodules of 1 cm or greater on dynamic CT or MRI scans who underwent pathologic confirmation at two university hospitals from August 2002 to February 2022. This group served as the test dataset. The primary outcome was the diagnostic performance of LR-5 for HCC using CT and MRI. When LI-RADS categorization differed between CT and MRI, the MRI-based classification was used as the definitive category. Results were validated using a dataset of patients with CHC from two additional hospitals based on the clinical composite reference standard. Sensitivity, specificity, and area under the receiver operating characteristic curve (AUC) were calculated.

Results: The test dataset comprised 458 patients (mean age, 64 years ± 9 [SD]; 350 male; 219 without cirrhosis, 239 with cirrhosis). For noncirrhotic livers, the LR-5 criteria achieved an AUC, accuracy, sensitivity, specificity, positive predictive value (PPV), and negative predictive value (NPV) of 0.90 (95% CI: 0.86, 0.93), 85.1% (95% CI: 80.6, 89.7), 82.4% (95% CI: 77.0, 87.8), 97.6% (95% CI: 93.0, 100.0), 99.4% (95% CI: 98.2, 100.0), and 54.7% (95% CI: 43.4, 65.9), respectively. The AUC for LR-5 observations in diagnosing HCC was higher in the noncirrhotic liver group compared with the cirrhotic liver group (AUC, 0.90 [95% CI: 0.86, 0.93] vs 0.79 [95% CI: 0.74, 0.84]; *P* = .002).The diagnostic performance of the LR-5 criteria for diagnosing HCC was also excellent in patients with noncirrhotic CHC in the validation dataset, which included 155 lesions from 103 patients (mean age, 68 years ± 12; 146 male). The AUC, accuracy, sensitivity, specificity, PPV, and NPV in the validation dataset were 0.91 (95% CI: 0.84, 0.97), 96.1% (95% CI: 93.1, 99.2), 82.9% (95% CI: 70.4, 95.3), 100%, 100%, and 95.2% (95% CI: 91.5, 99.0), respectively.

Conclusion: The diagnostic performance of LR-5 for HCC in patients with noncirrhotic CHC was comparable to that in patients with cirrhosis across various clinical settings.

© RSNA, 2025

Supplemental material is available for this article.

Long-lasting hepatic inflammation caused by the hepatitis C virus (HCV) often leads to the sequential development of advanced fibrosis, cirrhosis, and hepatocellular carcinoma (HCC) (1). However, evidence suggests that there is a 5-year risk of 1.35%–1.6% in patients with noncirrhotic chronic hepatitis C (CHC) in developing HCC, pointing to the occurrence of direct viral causation, possibly as a result of synergy between viral-induced oncogenic and host-related pathways (2,3). Moreover, curing HCV with antiviral treatment does not entirely eradicate the risk of HCC, even in patients without liver cirrhosis (LC) (4,5).

Current practice guidelines from various sources recommend diagnosing HCC via multiphasic CT or MRI without histologic confirmation in high-risk patients (6–9). These guidelines vary in their strictness and permissiveness. European guidelines do not consider individuals infected with hepatitis B virus or HCV but without LC as being high risk (7). In contrast, the Liver Imaging Reporting and Data System (LI-RADS) criteria and the most recent update from the American Association for the Study of Liver Diseases accept an imaging-based diagnosis of HCC without biopsy for LI-RADS category 5 (LR-5) lesions in patients with noncirrhotic hepatitis B virus (6,10). However, these LI-RADS-based imaging diagnosis criteria have not been validated in populations with noncirrhotic HCV infection.

Considering the importance of radiologic diagnosis in the context of HCC risk, this study aimed to evaluate the diagnostic performance of LR-5 observations for HCC using CT and MRI in patients with noncirrhotic CHC and to compare these findings with those in patients with CHC and cirrhosis.

Materials and Methods

Study Design and Patients

This retrospective investigation was conducted at four hospitals in the Republic of Korea (Asan Medical Center, Jeju University Hospital, Hanyang University Guri Hospital, and

Abbreviations

AUC = area under the receiver operating characteristic curve,
CHC = chronic hepatitis C, HCC = hepatocellular carcinoma,
HCV = hepatitis C virus, LC = liver cirrhosis, LI-RADS = Liver
Imaging Reporting and Data System, PPV = positive predictive value

Summary

Liver Imaging Reporting and Data System criteria demonstrated high
diagnostic accuracy for diagnosing hepatocellular carcinoma using CT
and MRI in patients with noncirrhotic chronic hepatitis C.

Key Results

- In this retrospective study of 458 patients with chronic hepatitis
  C, Liver Imaging Reporting and Data System (LI-RADS) category
  5 (LR-5) criteria demonstrated high diagnostic performance for
  hepatocellular carcinoma (HCC) in noncirrhotic livers using CT and
  MRI, with the area under the receiver operating characteristic curve
  (AUC) of 0.90 (95% CI: 0.86, 0.93), sensitivity of 82.4% (95% CI:
  77.0, 87.8), and specificity of 97.6% (95% CI: 93.0, 100.0).
- The AUC was higher in the noncirrhotic group than in the
  cirrhotic group (AUC, 0.90 [95% CI: 0.86, 0.93] vs 0.79 [95%
  CI: 0.74, 0.84]; P = .002).
- In the validation dataset of 103 patients with noncirrhotic chronic
  hepatitis C, LR-5 criteria maintained high diagnostic accuracy of
  96.1% (95% CI: 93.1, 99.2) for HCC.

Sanggye Paik Hospital). The requirement for informed consent was waived by the institutional review board of each institution. The study populations in both datasets were patients aged 20 years or older with CHC in different health care settings. CHC was defined by a positive anti-HCV antibody test and a history of viremia lasting more than 6 months, regardless of any anti-HCV treatment, which is in line with the international guidelines (11,12). The test dataset consisted of patients with CHC from the Asan Medical Center and Jeju University Hospital enrolled between January 2000 and February 2022. Inclusion criteria required that patients had at least one hepatic lesion measuring 1 cm or greater, which is recognized as the minimum nodule diameter for a noninvasive diagnosis of HCC (6,7,13,14), and underwent biopsy or surgical resection for histologic diagnosis of focal liver lesions. Exclusion criteria in the test dataset included the following: *(a)* coinfection with hepatitis B virus and/or HIV; *(b)* history of prior treatment for any intrahepatic cancer, including HCC; *(c)* those without histologic liver parenchyma specimens; *(d)* those in whom the interval between imaging and histopathologic examinations exceeded 3 months; or *(e)* those whose lesions were intraductal or poorly delineated.

To generalize the results from the test dataset to a broader population and minimize potential selection biases, a validation dataset consisting of patients with CHC was independently established at two secondary hospitals, Hanyang University Guri Hospital and Sanggye Paik Hospital, from March 2004 to December 2022. The inclusion criteria required that the patients have hepatic lesions measuring at least 1 cm at abdominal imaging. Exclusion criteria in the test dataset included the following: *(a)* coinfection with hepatitis B virus or HIV; *(b)* absence of lesions on dynamic contrast-enhanced CT or MRI scans; *(c)* lack of a definitive diagnosis; or *(d)* a history of prior treatment for any intrahepatic cancer, including HCC. Detailed information regarding study sample is available in Appendix S1.

Diagnostic Definitions of Underlying Liver Fibrosis

In the test dataset, liver histologic findings were scored according to the Meta-analysis of Histological Data in Viral Hepatitis, or METAVIR, classification of fibrosis stages (F0–F4, where F0 indicates no fibrosis; F1, portal fibrosis without septa; F2, portal fibrosis with few septa; F3, numerous septa without cirrhosis; and F4, cirrhosis) (15), based on either a resection specimen or biopsy. In the validation dataset, the presence of cirrhosis was decided by a composite definition in order of preference of *(a)* a pathologic report showing evidence of cirrhosis at resection; *(b)* a pathologic report with cirrhosis noted at biopsy; or *(c)* the presence of clinical, radiologic, endoscopic, or laboratory evidence of cirrhosis and/or portal hypertension (eg, irregular hepatic surface, esophageal or gastric varices, collaterals, recanalized umbilical vein, ascites, and splenomegaly) (16).

Image Protocol

All CT examinations were performed with an 8-, 16-, 64-, or 128-channel multidetector CT scanner. After unenhanced images had been acquired, contrast-enhanced images were obtained after intravenous injection of 1.5–2 mL/kg of body weight of iodinated contrast material (iopromide) at a rate of 3–4 mL/sec.

All MRI examinations were conducted with either a 1.5-T or 3.0-T scanner. The MRI protocol included unenhanced MRI sequences (T1-weighted dual gradient-echo in- and opposed-phase imaging, respiratory-triggered turbo spin-echo T2-weighted imaging, and diffusion-weighted imaging) and contrast-enhanced T1-weighted three-dimensional gradient-echo imaging after injection of contrast media (gadolinium ethoxybenzyl diethylenetriamine pentaacetic acid, gadobenate dimeglumine, or gadoterate meglumine). Detailed imaging parameters are presented in Appendix S1.

Image Analysis

All imaging studies were anonymized and independently reviewed by two board-certified abdominal radiologists (R.P. and S.H.C., with 5 and 10 years of experience, respectively) using a standardized LI-RADS reporting template. In cases of discrepancies between the two readers, the images were re-evaluated collaboratively, and a consensus was reached. To mitigate potential recall bias, CT images were reviewed in the first session, and MRI scans were reviewed in the second session. There was a 4-week interval between the two sessions.

For the imaging characteristics of the target lesions, the readers assessed lesion size and decided on the presence or absence of major features (such as nonrim arterial phase hyperenhancement, washout, an enhancing capsule, and threshold growth), ancillary features, and targetoid or nontargetoid features in accordance with LI-RADS version 2018 (10). When LI-RADS categorization differed between CT and MRI, the MRI-based observation was chosen as the final category due to the superior diagnostic accuracy of MRI LI-RADS for HCC (10,17).

Reference Standard for Lesions of Each LI-RADS Category

In the test dataset, pathology-based reference standards with histopathologic proof were used for all nodules. Positive histologic finding for HCC was considered only if the examination was performed within 3 months after the last imaging session. For the
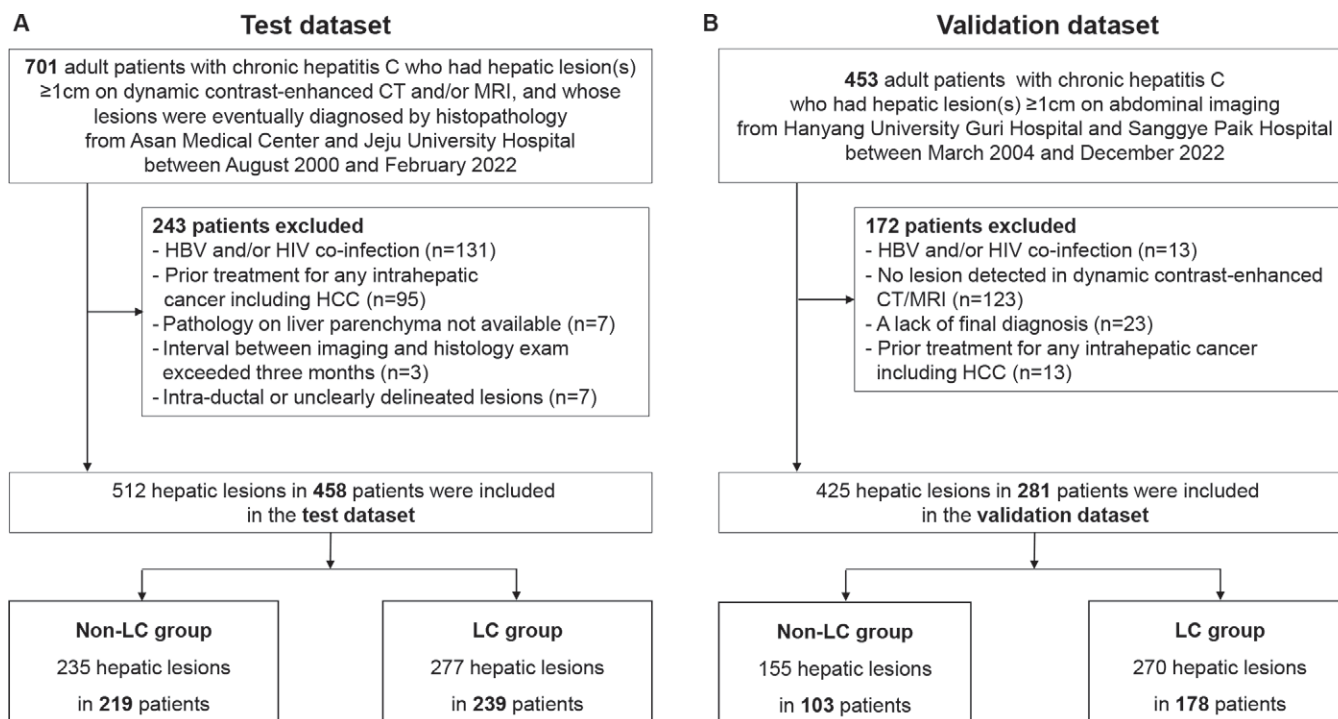
Figure 1: Flow diagram of patient enrollment in the **(A)** test dataset and **(B)** validation dataset. HBV = hepatitis B virus, HCC = hepatocellular carcinoma, LC = liver cirrhosis.

validation dataset, the primary diagnostic reference was pathologic examination. Composite clinical reference standards were adopted for the final diagnosis in nodules for which pathologic examination was unavailable, based on prior studies aiming to closely mirror daily practice (18–20). Detailed information regarding benign lesions and non-HCC malignancy is available in Appendix S1.

Statistical Analysis

Statistical analyses are detailed in Appendix S1. The diagnostic performance of imaging observations for detecting HCC was evaluated by calculating the accuracy, sensitivity, specificity, positive predictive value (PPV), negative predictive value, and area under the receiver operating characteristic curve (AUC). The DeLong test was used to compare the AUCs between models (21). Logistic regression analysis was used to examine the factors associated with LR-5 HCC.

To ascertain the required sample size in the test dataset, we employed the CI method using the exact Clopper-Pearson formula. Assuming an HCC prevalence of 80% within the noncirrhotic target population and based on a specificity of 0.9, a sensitivity of 0.7, and a precision of 0.02, we estimated that a sample size of 221 lesions was needed. Interreader agreement for LI-RADS category assessment was evaluated using Cohen κ statistic (22).

All statistical procedures were performed with R statistical software (version, 4.2.1; R Foundation for Statistical Computing; *http://cran.r-project.org*). A threshold of $P < .05$ was applied for statistical significance.

Results

Patient Characteristics

Of the 701 patients identified, 243 (34.7%) were excluded (Fig 1A). Finally, 458 patients diagnosed with CHC were included in the test dataset (Table 1). Diagnostic imaging methods included CT for 70 patients (15.3%, 70 of 458), MRI for 17 patients (3.7%, 17 of 458), and a combination of methods for 371 patients (81.0%, 371 of 458) (Table 2). Single lesions were detected in 413 patients (90.2%, 413 of 458). The median diameter of the largest nodules was 3.0 cm, with an IQR of 2.0–4.5 cm. Of the 458 patients, 129 (28.2%) had nodules measuring 2 cm or less in diameter. Histologic confirmation was obtained through surgical specimens from 426 patients, biopsy specimens from 11 patients, and a combination of both methods for 21 patients.

The study comprised 239 patients (52.2%, 239 of 458) with underlying F4 fibrosis, and they were classified into the LC group, while the remaining 219 patients (47.8%, 219 of 458) were classified into the non-LC group. The non-LC groups had a higher proportion of male patients (184 of 219 [84.0%] vs 166 of 239 [69.5%]; $P < .001$) and a larger diameter of the biggest lesion (3.4 cm vs 2.8 cm; $P < .001$). Diabetes mellitus was more common in the LC group (43 of 219 [19.6%] vs 90 of 239 [37.7%]; $P < .001$).

Imaging and Histopathologic Analysis

A total of 512 lesions from 458 patients underwent pathologic assessment. According to LI-RADS, 40 lesions were classified as LR-3 (7.8%), 84 as LR-4 (16.4%), 325 as LR-5 (63.5%), 45 as LR-M (8.8%), and 18 as LR-TIV (tumor in vein) (3.5%). LR-1 and LR-2 lesions were not included because pathologic examination of these lesions was not performed. Disagreement in LI-RADS category between CT and MRI occurred in 98 of 417 (23.5%) nodules visualized at both MRI and CT, which is similar to previous reports (Table S1) (18,23).

Interreader agreement for LI-RADS categorization showed κ of 0.82 (95% CI: 0.76, 0.87) for overall patients, 0.84 (95% CI: 0.78, 0.89) for the CT subgroup, and 0.84 (95% CI: 0.78, 0.90) for the MRI subgroup. At histopathologic examination,

Table 1: Demographic and Laboratory Characteristics of Patients in the Test Dataset

Characteristic	Entire Group (n = 458)	Non-LC (n = 219)	LC (n = 239)	P Value*
Demographic variable				
Age (y)				.07
Mean ± SD	64 ± 9	65 ± 8	63 ± 9	…
Median	64 (41–86)	65 (41–86)	64 (41–82)	…
Sex				<.001
Male	350 (76.4)	184 (84.0)	166 (69.5)	…
Female	108 (23.6)	35 (16.0)	73 (30.5)	…
Current smoking	131 (28.6)	57 (26.0)	74 (31.0)	.29
Current alcohol consumption	206 (45.0)	106 (48.4)	100 (41.8)	.19
Diabetes mellitus	133 (29.0)	43 (19.6)	90 (37.7)	<.001
Body mass index (kg/m^2)	24.2 (22.4–26.1)	23.8 (22.1–25.7)	24.6 (22.7–26.6)	.008
Body mass index ≥ 25 kg/m^2	189 (41.3)	81 (37.0)	108 (45.2)	.09
Laboratory findings				
AST level (IU/L)	49 (29–80)	35 (24–58)	65 (41–90)	<.001
ALT (IU/L)	35 (20–61)	30 (18–49)	42 (23–67)	.001
Total bilirubin level (mg/dL)	0.9 (0.6–1.3)	0.8 (0.6–1.1)	1.1 (0.7–1.6)	<.001
International normalized ratio	1.2 (1.1–1.3)	1.1 (1.1–1.2)	1.2 (1.1–1.3)	<.001
Albumin level (g/dL)	3.2 (2.8–3.6)	3.3 (3.0–3.7)	3.1 (2.6–3.5)	.001
Platelet count (×10^9/L)	149 (107–190)	167 (137–208)	120 (84–166)	<.001
AFP level (ng/mL)[†]	8.7 (3.5–41.1)	5.6 (2.7–27.9)	11.3 (4.8–46.6)	<.001
AFP ≥ 20 ng/mL[†]	150 (32.9)	61 (28.1)	89 (37.2%)	.049
HCV-related factor				
HCV RNA positive at lesion detection	282 (61.6)	126 (57.5)	156 (65.3)	.038
Previous treatment of HCV[‡]				.039
Direct-acting antiviral	131 (28.6)	62 (28.3)	69 (28.9)	…
Interferon	68 (14.8)	29 (13.2)	39 (16.3)	…
None	252 (55.0)	121 (55.3)	131 (54.8)	…
Unknown	7 (1.5)	7 (3.2)	…	…

Note.—Continuous data are presented as medians, with IQRs in parentheses. Categorical data are presented as numbers, with percentages in parentheses. Body mass index was calculated as weight in kilograms divided by height in meters squared. AFP = α-fetoprotein, ALT = alanine aminotransferase, AST = aspartate aminotransferase, HCV = hepatitis C virus, LC = liver cirrhosis.

* P values for comparison between noncirrhotic and cirrhotic groups were calculated using the χ^2 test or Fisher exact test for categorical variables and the t test or Mann-Whitney U test for continuous variables.

[†] AFP values at the time the lesions were detected were not available for two patients.

[‡] Of the patients treated for HCV, 84.9% (169 of 199) achieved a sustained virologic response.

434 lesions were classified as HCC (84.8%), 52 as other malignant lesions (10.2%), and 26 as benign lesions (5.1%). Of the 434 HCCs, 340 underwent gadoxetic acid–enhanced MRI: 261 showed nonrim arterial phase hyperenhancement and portal venous washout, 56 showed nonrim arterial phase hyperenhancement without portal venous washout but with hepatobiliary phase hypointensity, and 10 showed hepatobiliary phase hyperintensity.

A per-nodule analysis revealed that 325 of the nodules (63.5%) exhibited the typical enhancement pattern for HCC (ie, LR-5) on CT and/or MRI scans (Table 3). Of these, 321 (98.8%) were histopathologically confirmed as HCC: 159 of 160 (99.4%) in the non-LC group and 162 of 165 (98.2%) in the LC group. One hepatic lesion in the non-LC group, classified as LR-5 but not as HCC, was identified as combined hepatocellular-cholangiocarcinoma. In the LC group, three LR-5 lesions were diagnosed as follows: two as combined hepatocellular-cholangiocarcinoma and one as cholangiocarcinoma. In the non-LC and LC groups, actual HCCs constituted seven of 15

(46.7%) and 15 of 25 (60.0%), respectively, of the LR-3 nodules, 15 of 22 (68.2%) and 54 of 62 (87.1%), respectively, of the LR-4 nodules, four of 27 (14.8%) and four of 18 (22.2%), respectively, of the LR-M nodules, and eight of 11 (72.7%) and six of seven (85.7%), respectively, of the LR-TIV nodules.

When we examined the characteristics of the HCCs in noncirrhotic HCV-infected livers, we observed a higher prevalence of male patients and current alcohol consumption among the patients with HCC. Furthermore, F3 fibrosis, serum α-fetoprotein levels of 20 ng/mL or greater, and a history of anti-HCV therapy, particularly with direct-acting agents, were also more prevalent in the HCC group (Table S2). Figures 2 and S1 show a representative LR-5 HCC case in the non-LC group.

Further multivariable analysis indicated that a solitary tumor (adjusted odds ratio [OR], 2.32; 95% CI: 1.21, 4.47; P = .011) and larger tumor size (≥ 2 cm) (adjusted OR, 2.92; 95% CI: 1.89, 4.51; P < .001) were factors independently associated with HCCs meeting the LR-5 criteria in the 458 patients; however, there was no evidence of a difference in the presence of LC (OR,

Table 2: Imaging and Pathologic Characteristics of the Patients in the Test Dataset

Characteristic	Entire Group (n = 458)	Non-LC (n = 219)	LC (n = 239)	P Value*
Indication for dynamic imaging				.12
Surveillance setting	298 (65.1)	151 (68.9)	147 (61.5)	…
Nonsurveillance setting†	160 (34.9)	68 (31.1)	92 (38.5)	…
Type of dynamic imaging				.054
CT and MRI‡	371 (81.0)	174 (79.5)	197 (82.4)	…
CT alone	70 (15.3)	32 (14.6)	38 (15.9)	…
MRI alone‡	17 (3.7)	13 (5.9)	4 (1.7)	…
No. of lesions per patient				.019
One	413 (90.2)	203 (92.7)	210 (87.9)	…
Two	37 (8.1)	16 (7.3)	21 (8.8)	…
Three or more	8 (1.7)	…	8 (3.3)	…
Diameter of largest lesion (cm)	3.0 (2.0–4.5)§	3.4 (2.2–5.5)	2.8 (2.0–3.9)	<.001
≤2	129 (28.2)	47 (21.5)	82 (34.3)	.003
>2	329 (71.8)	172 (78.5)	157 (65.7)	…
Type of specimen for pathologic diagnosis				.19
Resection	426 (93.0)	199 (90.9)	227 (95.0%)	…
Biopsy	11 (2.4)	6 (2.7)	5 (2.1)	…
Biopsy and resection	21 (4.6)	14 (6.4)	7 (2.9)	…
Hepatic steatosis	168 (36.7)	55 (25.1)	113 (47.3)	<.001
METAVIR fibrosis score‖				<.001
F0	16 (3.5)	16 (7.3)	…	…
F1	37 (8.1)	37 (16.9)	…	…
F2	65 (14.2)	65 (29.7)	…	…
F3	101 (22.0)	101 (46.1)	…	…
F4	239 (52.2)	…	239 (100.0)	…

Note.—Continuous data are presented as medians, with IQRs in parentheses. Categorical data are presented as numbers, with percentages in parentheses. LC = liver cirrhosis, METAVIR = Meta-analysis of Histological Data in Viral Hepatitis.

* P values for comparison between noncirrhotic and cirrhotic groups were calculated using the χ^2 test or Fisher exact test for categorical variables, and the t test or Mann-Whitney U test for continuous variables.

† The indications for dynamic imaging in these patients included presence of symptoms (n = 54), incidental findings (n = 85), and abnormal liver function tests (n = 21).

‡ Among the 388 patients who underwent dynamic MRI, imaging was enhanced with gadolinium ethoxybenzyl diethylenetriamine pentaacetic acid (Gd-EOB-DTPA) in 355 (91.5%), gadobenate dimeglumine in 16 (4.1%), and gadoterate meglumine in 17 (4.4%).

§ The median sizes of the largest lesions in patients under surveillance and those from a nonsurveillance setting were 2.5 cm (range, 2.0–3.2 cm) and 5.3 cm (range, 3.8–7.8 cm), respectively (P < .001).

‖ F0 indicates no fibrosis; F1, portal fibrosis without septa; F2, portal fibrosis with few septa; F3, numerous septa without cirrhosis; and F4, cirrhosis.

0.76; 95% CI: 0.51, 1.12; P = .16), diabetes (OR, 0.74; 95% CI: 0.49, 1.13; P = .17), or hepatic steatosis (OR, 1.11; 95% CI: 0.75, 1.67; P = .60) (Table S3). The variance inflation factor for the variables in the multivariable regression model ranged from 1.00 to 1.02. The P value of Hosmer-Lemeshow test was .25, indicating goodness of fit.

Diagnostic Performance of LI-RADS 5 Imaging Criteria for HCC

For all lesions, the LI-RADS 5 criteria demonstrated the following diagnostic performance for HCC: accuracy of 77% (95% CI: 73.5, 80.8), sensitivity of 74% (95% CI: 69.8, 78.1), specificity of 95% (95% CI: 90.0. 99.8), PPV of 99% (95% CI: 97.6, 100.0), and negative predictive value of 40% (95% CI: 32.6, 46.6), as outlined in Table 4. For nodules in patients with noncirrhotic CHC, the corresponding values were 85% (95% CI: 80.6, 89.7), 82% (95% CI: 77.0, 87.8), 98% (95% CI: 93.0, 100.0), 99% (95% CI: 98.2, 100.0),

and 55% (95% CI: 43.4, 65.9). The diagnostic accuracy of the LR-5 observations remained consistent regardless of the presence of LC. Notably, the AUC was higher in the noncirrhotic group than in the cirrhotic group (0.90 [95% CI: 0.86, 0.93] vs 0.79 [95% CI: 0.74, 0.84]; P = .002). The LI-RADS 5 criteria also yielded a high Nagelkerke R^2 value of 0.59 and a low Brier score of 0.15 in patients with noncirrhotic CHC. The diagnostic performance of LR-5 and LR-TIV nodules for HCC diagnosis according to the presence of LC was similar to the results of LR-5 only (Table S4).

Tables 5 and S5 provide stratified analyses based on factors that include the stage of liver fibrosis, imaging modality, type of contrast agent, and obesity, defined as body mass index of 25 kg/m² or greater in Asian populations. There was no evidence of a difference in the diagnostic performance. The AUCs were greater than 0.80 across these subgroups in the non-LC group, except for patients with F0–F1 fibrosis compared with those with F2 fibrosis (AUC, 0.96 vs 0.84; P = .037).

Table 3: LI-RADS and Histopathologic Characteristics of Hepatic Lesions according to Presence of LC in the Test Dataset

Pathologic Diagnosis	All Lesions	LI-RADS Category									
		Lesions in Non-LC (n = 235)					Lesions in LC (n = 277)				
		LR-3	LR-4	LR-5	LR-M	LR-TIV	LR-3	LR-4	LR-5	LR-M	LR-TIV
No. of lesions	512	15 (6.4)	22 (9.4)	160 (68.1)	27 (11.4)	11 (4.7)	25 (9.0)	62 (22.4)	165 (59.6)	18 (6.5)	7 (2.5)
Diameter of largest lesion (cm)	3.0 (2.0–4.2)	1.8 (1.3–2.4)	2.6 (2.0–5.0)	3.2 (2.3–5.8)	3.4 (2.0–5.2)	4.0 (3,2–6.4)	1.5 (1.0–2.0)	2.0 (1.7–3.0)	3.0 (2.0–4.0)	2.6 (2.0–3.4)	6.0 (4.0–8.1)
HCC	434 (84.8)	7 (46.7)	15 (68.2)	159 (99.4)	4 (14.8)	8 (72.7)	15 (60.0)	54 (87.1)	162 (98.2)	4 (22.2)	6 (85.7)
Other malignant lesion	52 (10.2)	1 (6.7)	7 (31.8)	1 (0.6)	21 (77.8)	3 (27.3)	…	3 (4.8)	3 (1.8)	12 (66.7)	1 (14.3)
Combined HCC-CCA	13	…	2	1	3	…	…	2	2	3	…
Intrahepatic CCA	21	1	2	…	6	2	…	1	1	7	1
Metastatic cancer	18	…	3	…	12	1	…	…	…	2	…
Benign lesion	26 (5.1)	7 (46.7)	…	…	2 (7.4)	…	10 (40.0)	5 (8.1)	…	2 (11.1)	…
Angiomyolipoma	1	…	…	…	1	…	…	…	…	…	…
Inflammatory nodule	2	2	…	…	…	…	…	…	…	…	…
Hepatic cyst	3	3	…	…	…	…	…	…	…	…	…
Eosinophilic granuloma	1	1	…	…	…	…	…	…	…	…	…
Hemangioma	2	1	…	…	1	…	…	…	…	…	…
Dysplastic nodule	13	…	…	…	…	…	8	5	…	…	…
Regenerative nodule	4	…	…	…	…	…	2	…	…	2	…

Note.—Continuous data are presented as medians, with IQRs in parentheses. Categorical data are presented as numbers, with percentages in parentheses. CCA = cholangiocarcinoma, HCC-CCA = combined hepatocellular-CCA, LC = liver cirrhosis, LI-RADS = Liver Imaging Reporting and Data System, TIV = tumor in vein.

Evaluating Pretest and Posttest Probabilities of LR-5 HCC in Patients with Noncirrhotic CHC

Figure 3 showcases a Fagan nomogram, delineating the shift in pretest to posttest probabilities of HCC after receipt of positive versus negative LR-5 results. Given the average prevalence of 82.1% in the test sample, the positive likelihood ratio would yield a posttest probability for HCC of 99% for an LR-5 result. However, a negative LR-5 outcome reduced this likelihood dramatically to 42%. Further exploration of how pretest probability influences the LI-RADS 5 criteria in settings of varying HCC prevalence is shown in Table S6. For instance, when the pretest probabilities stood at 40% and 60% and the LR-5 criteria were met, the resulting posttest probabilities soared to 96% and 98%, respectively.

Validation Dataset Results

Of the 453 patients identified, 172 (35%) were excluded (Fig 1B). The baseline characteristics of 281 patients in the validation dataset, including 103 without LC and 178 with LC, are detailed in Table S7.

A per-nodule analysis included a total of 425 lesions, of which 155 were in noncirrhotic livers and 270 were in cirrhotic livers (Table S8). In terms of the method used for diagnosing hepatic lesions, 48 of 425 (11%) were identified at histopathologic examination and 377 of 425 (89%) by using a clinical composite reference standard, with no evidence of a difference according to the presence of LC (P = .75). According to the LI-RADS classification, 154 lesions were categorized as LR-1

(36%), 15 as LR-2 (3.5%), 21 as LR-3 (5%), eight as LR-4 (2%), 176 as LR-5 (41%), 20 as LR-M (5%), and 31 as LR-TIV (7%). The final assignment of the lesions was HCC in 212 (50%), other malignant lesions excluding HCC in 18 (4%), and benign lesions in 195 (46%). The prevalence of HCC was 23% (35 of 155) in patients without LC and 66% (177 of 270) in patients with LC.

Regarding the diagnostic performance of LR-5 for HCC in patients with noncirrhotic CHC, the accuracy, sensitivity, specificity, PPV, and negative predictive value were 85%, 82%, 98%, 99%, and 55% respectively, as shown in Table S9. There was no evidence of a difference between the AUC for the non-LC group and the LC group (AUC, 0.91 [95% CI: 0.84, 0.97] vs 0.92 [95% CI: 0.89, 0.94]; P = .98); the former had a higher Nagelkerke R^2 value (0.809 vs 0.749) and a lower Brier score (0.039 vs 0.111). The diagnostic performance of LR-5 and LR-TIV nodules for HCC diagnosis, according to the presence of LC, is presented in Table S10. There was no evidence of a difference in diagnostic performance according to the imaging modality in the non-LC group of validation dataset (Table S11).

Discussion

This study evaluated the performance of Liver Imaging Reporting and Data System (LI-RADS) category 5 (LR-5) criteria using CT and MRI for diagnosing hepatocellular carcinoma (HCC) in patients with noncirrhotic chronic hepatitis C (CHC) across different HCC prevalence settings. The
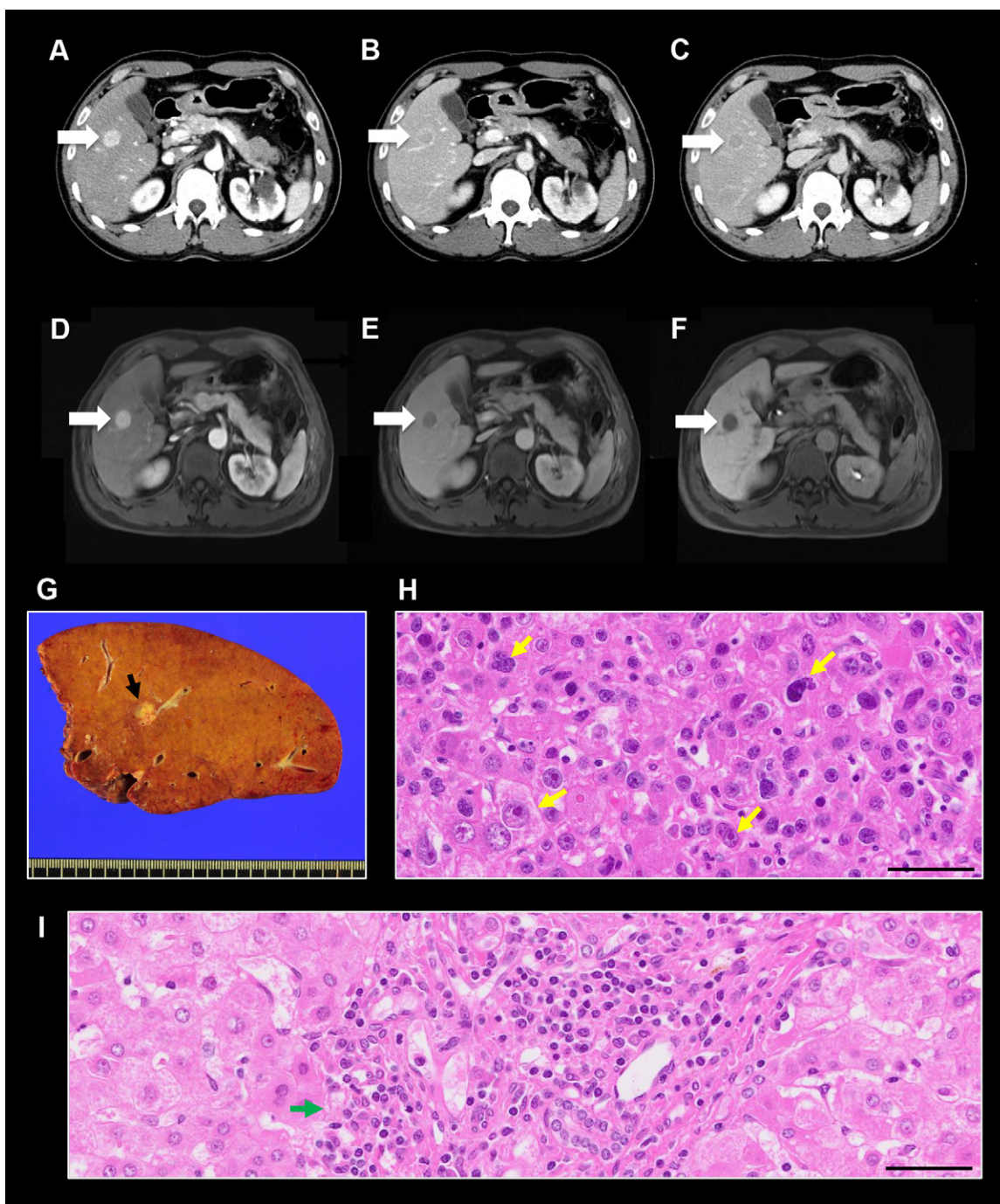
Figure 2: Images in a 46-year-old male patient with chronic hepatitis C without liver cirrhosis undergoing biannual hepatocellular carcinoma (HCC) surveillance. Because of the risk of tumor seeding, surgical resection was performed without prior biopsy. **(A–C)** Multiphase contrast-enhanced CT scans show a 2.0-cm arterial phase hyperenhancing mass in segment V **(A)**, with enhancing capsule on portal venous phase **(B)** and washout on delayed phase image **(C)**. **(D–F)** Gadoxetic acid–enhanced MRI scans also show **(D)** arterial phase hyperenhancement, **(E)** portal venous washout, and **(F)** hepatobiliary phase hypointensity. This mass (arrow) was classified as Liver Imaging Reporting and Data System category 5 at both CT and MRI and was surgically confirmed as HCC. **(G)** Photograph of the cut surface of the resected specimen. The tumor (black arrow) appears yellow and round, measuring 1.0 cm in its maximum dimension. **(H)** Photomicrograph shows highly pleomorphic tumor cells (yellow arrows), consistent with poorly differentiated HCC. (Hematoxylin-eosin stain; original magnification, ×400.) **(I)** Background liver parenchyma shows moderate portal inflammation (green arrow) without evidence of cirrhosis. (Hematoxylin-eosin stain; original magnification, ×400.) Scale bar = 50 μm.

investigation demonstrated high accuracy, with specificity of 97.6% and positive predictive value (PPV) of 99.4% for HCC diagnosis in rigorously defined patients with noncirrhotic CHC with complete histologic data. The high proportion of single lesions in our test dataset (90% of patients) provided a near one-to-one correspondence between image-detected lesions and resected specimens, enhancing the reliability of the radiologic-pathologic correlation. These findings were consistent even in patients with F0–F2 fibrosis, who are not typically considered candidates for HCC surveillance according to

Table 4: Performance of LR-5 Criteria in the Per-Lesion Diagnosis of HCC according to Presence of LC in the Test Dataset

Parameter	Total (n = 512)	Non-LC (n = 235)	LC (n = 277)
Accuracy (%)	77.2 (73.5–80.8)	85.1 (80.6–89.7)	70.4 (65.0–75.8)
Sensitivity (%)	74.0 (69.8–78.1)	82.4 (77.0–87.8)	67.2 (61.3–73.2)
Specificity (%)	94.9 (90.0–99.8)	97.6 (93.0–100.0)	91.7 (82.6–100.0)
AUC*	0.84 (0.81–0.88)	0.90 (0.86–0.93)	0.79 (0.74–0.84)
Likelihood ratio positive	14.42 (11.38–18.28)	34.60 (25.27–47.38)	8.07 (5.64–11.54)
Likelihood ratio negative	0.27 (0.24–0.31)	0.18 (0.15–0.21)	0.36 (0.30–0.43)
PPV (%)	98.8 (97.6–100.0)	99.4 (98.2–100.0)	98.2 (96.1–100.0)
NPV (%)	39.6 (32.6–46.6)	54.7 (43.4–65.9)	29.5 (21.0–37.9)
Brier score	0.229	0.149	0.296
Nagelkerke R^2 value	0.424	0.593	0.297

Note.—AUC = area under the receiver operating characteristic curve, HCC = hepatocellular carcinoma, LC = liver cirrhosis, NPV = negative predictive value, PPV = positive predictive value.
* P values with the DeLong test = .002.

international guidelines (6,12). In our noncirrhotic validation dataset with a prevalence of HCC likely to be encountered in routine practice, the PPV and specificity of LR-5 HCC nodules were also close to 100%, although this does not entirely exclude the possibility of combined hepatocellular-cholangiocarcinoma when using composite clinical reference. The higher negative predictive value for LR-5 in the validation dataset compared with the test set was primarily due to the inclusion of LR-1 and LR-2 lesions. Furthermore, modeling of the test performance demonstrated that the PPV was excellent—above 95%—across a range of pretest probabilities.

Most clinical practice guidelines worldwide allow noninvasive diagnosis of HCC in high-risk individuals (6,7,9). Although evidence supports the growing role of histoprognostic factors and molecular biology in prognosis and clinical decision-making, biopsies of liver tumors present potential risks (9,24). Instances of bleeding and needle track seeding are relatively rare and typically manageable (25), but challenges include targeting lesions in difficult areas of the liver, distinguishing lesions from nodular backgrounds, and the low sensitivity of biopsies—especially for tumors less than 2 cm (26,27). Our study provides evidence supporting the inclusion of patients with noncirrhotic HCV as an indication for the use of noninvasive LI-RADS criteria.

The diagnostic performances of noncirrhosis in our test and validation datasets were on a par with those observed in patients with cirrhosis. In theory, for a diagnostic test to effectively bypass biopsy, its PPV and specificity should be close to 100% to minimize false-positive findings (28). It is well-known that LC, irrespective of its cause, is a potential risk factor for non-HCC hepatic malignancies such as cholangiocarcinoma and combined hepatocellular-cholangiocarcinoma (29,30). It was therefore not surprising to find that the cirrhotic group in the test sample had a lower per-observation accuracy (AUC, 0.90 vs 0.79; P = .002 with DeLong test; LR positivity, 34.60 vs 8.07) for LR-5 HCCs, with 1.8% of the category including cancers with cholangiocarcinoma disease. Factors such as hepatic steatosis, diabetes mellitus, male sex, higher degree of fibrosis, and HCV viremia, which have been linked to an elevated risk of HCC (5,28), did not influence the diagnostic performance of LR-5 for noncirrhotic HCC. Further analyses revealed that neither lower nodule size (≤2 cm) nor MRI method—both of which potentially influence LI-RADS imaging sensitivity (17,18)—affected the outcomes. On the other hand, the diagnostic results for LR-5 HCC in our two LC datasets were consistent with prior data from populations with cirrhosis affected by various diseases (18,31,32). This consistency underscores the reliability of our performance metrics.

Crucially, it is reported that up to 20% of all HCCs originate in noncirrhotic backgrounds, including those infected with HCV. These often manifest with typical histopathologic and radiologic features (33,34). Even patients with HCV in whom the disease has not progressed to LC, or those who have experienced LC regression after antiviral treatment, still have a heightened risk of developing HCC compared with the general population—albeit a somewhat lower risk than individuals with concurrent LC (5,35). Given the remarkably high rates of HCV clearance achieved by contemporary antiviral therapies (11,12), moving forward, the ability to diagnose HCC accurately and noninvasively will likely become increasingly critical for cured patients without LC. However, the direct oncogenic mechanisms exerted by HCV proteins—over and above the progressive effects of chronic liver inflammation (33,36)—remain elusive.

In our test dataset, 321 of the 434 (74.0%) actual HCCs were classified as LR-5, and among patients without cirrhosis but with HCC, 159 of 193 (82.4%) were classified as LR-5. These values align with previous findings that assessed typical HCCs based on the European Association for the Study of the Liver, or EASL, radiologic criteria, notably nonrim arterial phase hyperenhancement and either portal venous or delayed washout (7). The LI-RADS system, which has gained superior recognition over other imaging criteria, stipulates that liver nodules in the LR-3, LR-4, LR-M, and LR-TIV categories (excluding LR-5) should be recommended for biopsy (10). This recommendation is driven by the perceived insufficient pretest ability of imaging alone to provide a conclusive diagnosis of malignancy.

Few other studies have explored the diagnostic accuracy of LI-RADS for HCC in patients with CHC but without LC. A nonconsecutive study by Ludwig et al (37), which evaluated the LI-RADS version 2018 criteria for the diagnosis of HCC among primary liver cancers of hepatocellular and/or cholangiocellular origin in 131 patients with noncirrhotic disorders—including six carriers of HCV—reported that LR-5 was highly specific (97%–100%). This striking observation might

Table 5: Performance of LI-RADS 5 Criteria for Per-Lesion Diagnosis of HCC according to Fibrosis Stage and Imaging Modality in the Non-LC Group of the Test Dataset

Parameter	F0–F1 (n = 56)	F2 (n = 67)	F3 (n = 112)	CT (n = 221)	MRI (n = 203)	MRI with Gd-EOB-DTPA (n = 179)	MRI with Extracellular Contrast Agents (n = 24)
Accuracy (%)	96.4 (91.6–100.0)	83.6 (74.7–92.5)	80.4 (73.0–87.7)	79.6 (74.3–85.0)	84.7 (79.8–89.7)	85.5 (80.3–90.6)	79.2 (62.9–95.4)
Sensitivity (%)	94.1 (86.2–100.0)	79.6 (68.9–90.4)	80.0 (72.4–87.7)	77.2 (71.1–83.2)	81.9 (76.1–87.8)	83.7 (77.8–89.5)	61.5 (35.1–88.0)
Specificity (%)	100.0	100.0	85.7 (59.8–100.0)	91.9 (83.1–100.0)	97.3 (92.1–100.0)	96.2 (88.8–100.0)	100.0
AUC	0.97 (0.93–1.00)	0.90 (0.83–0.94)	0.83 (0.69–0.93)	0.85 (0.79–0.89)	0.90 (0.86–0.93)	0.90 (0.85–0.94)	0.81 (0.65–0.92)
Likelihood ratio positive	Not estimable*	Not estimable*	5.60 (2.50–12.55)	9.52 (6.72–13.48)	30.31 (21.66–42.42)	21.75 (14.59–32.43)	NE*
Likelihood ratio negative	0.06 (0.04–0.08)	0.20 (0.15–0.27)	0.23 (0.16–0.34)	0.25 (0.21–0.30)	0.19 (0.16–0.22)	0.17 (0.14–0.21)	0.38 (0.19–0.77)
PPV (%)	100.0	100.0	98.8 (96.5–100.0)	97.9 (95.6–100.0)	99.3 (97.8–100.0)	99.2 (97.7–100.0)	100.0
NPV (%)	91.7 (80.6–100.0)	54.2 (34.2–74.1)	22.2 (6.5–37.9)	44.7 (33.6–55.9)	54.6 (42.5–66.6)	50.0 (36.1–63.9)	68.8 (46.0–91.5)
No. of LR-5 nodules	32	43	85	152	137	129	8
HCC at pathologic examination of LR-5 nodule (%)	100.0	100.0	98.8	99.3	99.3	99.2	100.0

Note.—Data in parentheses are 95% CIs. *P* values according to the DeLong test for two receiver operating characteristic (ROC) curves are as follows: F0–F1 versus F2, *P* = .037; F2 versus F3, *P* = .38; F0–F1 versus F3, *P* = .067; CT versus MRI, *P* = .14; MRI with Gd-EOB-DTPA versus MRI with extracellular contrast agents, *P* = .23. AUC = area under the ROC curve, Gd-EOB-DTPA = gadolinium ethoxybenzyl diethylenetriamine pentaacetic acid, HCC = hepatocellular carcinoma, LC = liver cirrhosis, LI-RADS = Liver Imaging Reporting and Data System, NPV = negative predictive value, PPV = positive predictive value.
* Cannot be estimated due to a specificity of 100%.

be attributed to the fact that only the three malignant pathologic conditions were included, not benign neoplasms. In a recent U.S. pivotal cross-sectional study, where LR-5 or LR-TIV is taken as diagnostic for HCC, those criteria confirmed HCC with a specificity of 81.5% and PPV of 93.4% in 338 focal lesions from noncirrhotic hepatitis B virus livers (38). The prevalence of HCC nodules in this cohort was 76%. These values are comparable to those of our HCV dataset without LC. Based on these findings, the American Association for the Study of Liver Diseases no longer requires histologic confirmation for LR-5 hepatic nodules in patients with noncirrhotic hepatitis B virus with a high pretest probability (6). Indeed, in several studies the probability of LR-5 indicating HCC ranged from 95% to 99% in patients with LC, regardless of etiology (18,31,32). Therefore, biopsies might also be avoidable when diagnosing LR-5 HCC in HCV cases without LC.

Our study had some limitations. First, its retrospective design imposes inherent constraints, underscoring the need for prospective investigations with a protocol-based diagnostic work-up of nodules. The ultimate benefit associated with the relevant use of LI-RADS criteria should be tested in such a population. Second, despite the large number of patients, and because our study was performed in a racially homogeneous Asian dataset, it needs to be validated in other racial populations to ensure the generalizability of the results. Third, the long

(20-year) study period may have introduced bias due to evolving CT and/or MRI technology. However, this effect is likely to have been minimal as most examinations (> 80%) in the dataset as a whole were performed after 2010, and the large sample size should have helped to mitigate potential inconsistencies. Fourth, the lack of an independent central imaging review could introduce potential bias. To mitigate this, the readers were blinded to histopathologic findings and clinical data, including prior interpretations or clinical outcomes. Additionally, imaging analyses for CT and MRI were conducted separately with a 4-week interval between them.

In conclusion, Liver Imaging Reporting and Data System category 5 (LR-5) demonstrated exemplary performance in diagnosing hepatocellular carcinoma (HCC) in patients without cirrhosis with persistent or cured hepatitis C virus infection, consistent across various HCC prevalence settings. These findings suggest that individuals with noncirrhotic chronic hepatitis C (CHC) may be candidates for imaging-based diagnosis of LR-5 HCC. Future prospective studies are needed to confirm these results and further evaluate the use of imaging criteria in cases with noncirrhotic CHC, especially when biopsy is not feasible.

Deputy Editor: Kathryn Fowler
Scientific Editor: Elizabeth Weintraub
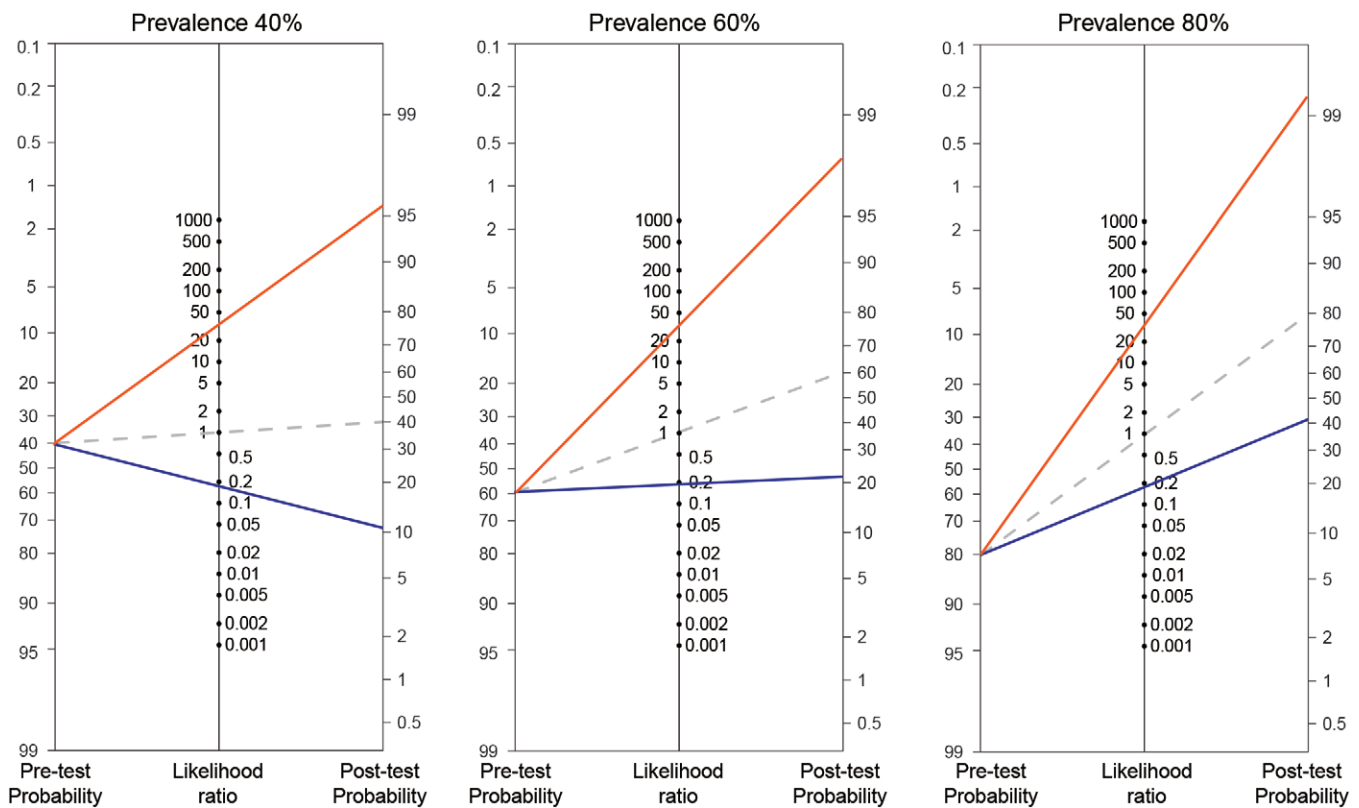
Figure 3: Pre- and posttest probabilities, along with likelihood ratios, of hepatocellular carcinoma (HCC) according to Liver Imaging Reporting and Data System (LI-RADS) category 5 (LR-5) criteria. Fagan nomogram was used to calculate posttest probabilities of HCC based on LR-5 criteria, assuming theoretical pretest probabilities of 40%, 60%, and 80% in patients with noncirrhotic chronic hepatitis C, using the diagnostic performance data from the test dataset. The orange line indicates the posttest probability if the test is positive; the blue line indicates the posttest probability if the test is negative; dotted gray line indicates he posttest probability when the test provides no diagnostic value (likelihood ratio = 1).

Author affiliations:

[1] Department of Gastroenterology and Hepatology, Hanyang University College of Medicine, Guri, Republic of Korea

[2] Department of Radiology and Research Institute of Radiology, University of Ulsan College of Medicine, Asan Medical Center, Seoul, Republic of Korea

[3] Department of Gastroenterology, Asan Medical Center, University of Ulsan College of Medicine, 88 Olympic-ro 43-gil, Songpa-gu, Seoul 05505, Republic of Korea

[4] Department of Internal Medicine, Jeju National University School of Medicine, Jeju, Republic of Korea

[5] Department of Gastroenterology, Inje University Sanggye Paik Hospital, Seoul, Republic of Korea

[6] Department of Pathology, Asan Medical Center, University of Ulsan College of Medicine, Seoul, Republic of Korea

[7] Asan Liver Center, Asan Medical Center, University of Ulsan College of Medicine, Seoul, Republic of Korea

[8] Department of Radiology, Hanyang University College of Medicine, Guri, Republic of Korea

[9] Department of Biostatistics, Korea University College of Medicine, Seoul, Republic of Korea

[10] Centre de Recherche des Cordeliers, Sorbonne Université, Inserm, Université de Paris Cité, team Functional Genomics of Solid Tumors, Equipe labellisée Ligue Nationale Contre le Cancer, Labex OncoImmunology, Paris, France

[11] Service d'hépatologie, Hôpital Avicenne, Hôpitaux Universitaires Paris-Seine-Saint-Denis, Assistance-Publique Hôpitaux de Paris, Bobigny, France

[12] Unité de Formation et de Recherche Santé Médecine et Biologie Humaine, Université Paris nord, Bobigny, France

Address correspondence to: J.H.S. (email: s5854@amc.seoul.kr).

Author contributions: Guarantors of integrity of entire study, **J.A., E.K., H.I.K., H.C.L., J.H.S.**; study concepts/study design or data acquisition or data analysis/interpretation, all authors; manuscript drafting or manuscript revision for important intellectual content, all authors; approval of final version of submitted manuscript, all authors; agrees to ensure any questions related to the work are appropriately resolved, all authors; literature research, **J.A., R.P., E.K., S.K.N., H.I.K., S.H.C., J.H.S.**; clinical studies, **J.A., R.P., E.K., S.K.N., H.I.K., I.H.S., J.H.K., H.C.L., J.C.N., S.H.C., J.H.S.**; experimental studies, **E.K., Y.S.C., J.H.S.**; statistical analysis, **J.A., E.K., S.K.N., H.I.K., S.H., S.H.C., J.H.S.**; and manuscript editing, **J.A., R.P., E.K., S.K.N., H.I.K., Y.S.C., H.C.L., S.H.C., J.H.S.**

Disclosures of conflicts of interest: J.A. No relevant relationships. **R.P.** No relevant relationships. **E.K.** No relevant relationships. **S.K.N.** No relevant relationships. **H.I.K.** No relevant relationships. **I.H.S.** No relevant relationships. **Y.S.C.** No relevant relationships. **J.H.K.** No relevant relationships. **H.C.L.** No relevant relationships. **S.H.** No relevant relationships. **J.C.N.** Research grants from Bayer and Ipsen; patents planned, issued, or pending from Brevet européen N°12306145.9 et américain N° 61/714,383 "A New Method for Classification of Liver Samples and Diagnosis of Focal Nodule Dysplasia, Hepatocellular Adenoma, and Hepatocellular Carcinoma;" Brevet européen N°12306146.7 et américain N° 61/704,360 "A New Method for Prognosis of Global Survival and Survival without Relapse in Hepatocellular Carcinoma;" Brevet européen B01811/WO-US; Réf. IT : BIO18522 et américain Demande de brevet US n° 17/605,524 "New Adeno-associated Virus (AAV) Variants and Uses Thereof for Gene Therapy;" Brevet européen PCT/FR2024/050073 "Methods of Predicting the Risk of Recurrence and/or Death of Patients Suffering from a Hepatocellular Carcinoma (HCC)." **S.H.C.** No relevant relationships. **J.H.S.** No relevant relationships.

References

1. Mezzacappa C, Kim NJ, Vutien P, Kaplan DE, Ioannou GN, Taddei TH. Screening for Hepatocellular Carcinoma and Survival in Patients With Cirrhosis After Hepatitis C Virus Cure. JAMA Netw Open 2024;7(7):e2420963.

2. Tanaka Y, Ogawa E, Huang CF, et al. HCC risk post-SVR with DAAs in East Asians: findings from the REAL-C cohort. Hepatol Int 2020;14(6): 1023–1033.

3. Leal C, Strogoff-de-Matos J, Theodoro C, et al. Incidence and Risk Factors of Hepatocellular Carcinoma in Patients with Chronic Hepatitis C Treated with Direct-Acting Antivirals. Viruses 2023;15(1):221.

4. Minami T, Sato M, Toyoda H, et al. Machine learning for individualized prediction of hepatocellular carcinoma development after the eradication of hepatitis C virus with antivirals. J Hepatol 2023;79(4):1006–1014.

5. Kanwal F, Kramer JR, Asch SM, Cao Y, Li L, El-Serag HB. Long-Term Risk of Hepatocellular Carcinoma in HCV Patients Treated With Direct Acting Antiviral Agents. Hepatology 2020;71(1):44–55.

6. Singal AG, Llovet JM, Yarchoan M, et al. AASLD Practice Guidance on prevention, diagnosis, and treatment of hepatocellular carcinoma. Hepatology 2023;78(6):1922–1965.

7. European Association for the Study of the Liver. EASL Clinical Practice Guidelines: Management of hepatocellular carcinoma. J Hepatol 2018;69(1):182–236. [Published correction appears in J Hepatol 2019;70(4):817.]

8. Omata M, Cheng AL, Kokudo N, et al. Asia-Pacific clinical practice guidelines on the management of hepatocellular carcinoma: a 2017 update. Hepatol Int 2017;11(4):317–370.

9. Korean Liver Cancer Association (KLCA) and National Cancer Center (NCC) Korea. 2022 KLCA-NCC Korea practice guidelines for the management of hepatocellular carcinoma. Clin Mol Hepatol 2022;28(4):583–705.

10. Chernyak V, Fowler KJ, Kamaya A, et al. Liver Imaging Reporting and Data System (LI-RADS) Version 2018: Imaging of Hepatocellular Carcinoma in At-Risk Patients. Radiology 2018;289(3):816–830.

11. Bhattacharya D, Aronsohn A, Price J, Lo Re V; AASLD-IDSA HCV Guidance Panel. Hepatitis C Guidance 2023 Update: AASLD-IDSA Recommendations for Testing, Managing, and Treating Hepatitis C Virus Infection. Clin Infect Dis 2023. 10.1093/cid/ciad319. Published online May 25, 2023.

12. European Association for the Study of the Liver. Electronic address: easloffice@easloffice.eu; Clinical Practice Guidelines Panel: Chair; EASL Governing Board representative; Panel members. EASL recommendations on treatment of hepatitis C: Final update of the series★. J Hepatol 2020;73(5):1170–1218. [Published correction appears in J Hepatol 2023;78(2):452.]

13. American College of Radiology. CT/MRI LI-RADS version 2018. https://www.acr.org/Clinical-Resources/Reporting-and-Data-Systems/LI-RADS/CT-MRI-LI-RADS-v2018. Accessed Feb 14, 2024.

14. Suddle A, Reeves H, Hubner R, et al. British Society of Gastroenterology guidelines for the management of hepatocellular carcinoma in adults. Gut 2024;73(8):1235–1268.

15. Poynard T, Bedossa P, Opolon P. Natural history of liver fibrosis progression in patients with chronic hepatitis C. The OBSVIRC, METAVIR, CLINIVIR, and DOSVIRC groups. Lancet 1997;349(9055):825–832.

16. Yoon JH, Kim YK, Kim JW, et al. Comparison of Four Diagnostic Guidelines for Hepatocellular Carcinoma Using Gadoxetic Acid-enhanced Liver MRI. Radiology 2024;311(1):e233114.

17. Roberts LR, Sirlin CB, Zaiem F, et al. Imaging for the diagnosis of hepatocellular carcinoma: A systematic review and meta-analysis. Hepatology 2018;67(1):401–421.

18. Ronot M, Fouque O, Esvan M, Lebigot J, Aubé C, Vilgrain V. Comparison of the accuracy of AASLD and LI-RADS criteria for the non-invasive diagnosis of HCC smaller than 3 cm. J Hepatol 2018;68(4):715–723.

19. van der Pol CB, McInnes MDF, Salameh JP, et al. CT/MRI and CEUS LI-RADS Major Features Association with Hepatocellular Carcinoma: Individual Patient Data Meta-Analysis. Radiology 2022;302(2):326–335.

20. Choi SJ, Choi SH, Kim DW, et al. Value of threshold growth as a major diagnostic feature of hepatocellular carcinoma in LI-RADS. J Hepatol 2023;78(3):596–603.

21. DeLong ER, DeLong DM, Clarke-Pearson DL. Comparing the areas under two or more correlated receiver operating characteristic curves: a nonparametric approach. Biometrics 1988;44(3):837–845.

22. McHugh ML. Interrater reliability: the kappa statistic. Biochem Med (Zagreb) 2012;22(3):276–282.

23. Cha DI, Jang KM, Kim SH, Kang TW, Song KD. Liver Imaging Reporting and Data System on CT and gadoxetic acid-enhanced MRI with diffusion-weighted imaging. Eur Radiol 2017;27(10):4394–4405.

24. Lehrich BM, Zhang J, Monga SP, Dhanasekaran R. Battle of the biopsies: Role of tissue and liquid biopsy in hepatocellular carcinoma. J Hepatol 2024;80(3):515–530.

25. Neuberger J, Patel J, Caldwell H, et al. Guidelines on the use of liver biopsy in clinical practice from the British Society of Gastroenterology, the Royal College of Radiologists and the Royal College of Pathology. Gut 2020;69(8): 1382–1403.

26. Singal AG, Ghaziani TT, Mehta N, et al. Recall patterns and risk of primary liver cancer for subcentimeter ultrasound liver observations: a multicenter study. Hepatol Commun 2023;7(3):e0073.

27. Müllhaupt B, Durand F, Roskams T, Dutkowski P, Heim M. Is tumor biopsy necessary? Liver Transpl 2011;17(Suppl 2):S14–S25.

28. Lee HC. Noninvasive diagnostic criteria for hepatocellular carcinoma. Clin Mol Hepatol 2012;18(2):174–177.

29. Clements O, Eliahoo J, Kim JU, Taylor-Robinson SD, Khan SA. Risk factors for intrahepatic and extrahepatic cholangiocarcinoma: A systematic review and meta-analysis. J Hepatol 2020;72(1):95–103.

30. Kalaitzakis E, Gunnarsdottir SA, Josefsson A, Björnsson E. Increased risk for malignant neoplasms among patients with cirrhosis. Clin Gastroenterol Hepatol 2011;9(2):168–174.

31. Kim YY, An C, Kim S, Kim MJ. Diagnostic accuracy of prospective application of the Liver Imaging Reporting and Data System (LI-RADS) in gadoxetate-enhanced MRI. Eur Radiol 2018;28(5):2038–2046.

32. van der Pol CB, Lim CS, Sirlin CB, et al. Accuracy of the Liver Imaging Reporting and Data System in Computed Tomography and Magnetic Resonance Image Analysis of Hepatocellular Carcinoma or Overall Malignancy-A Systematic Review. Gastroenterology 2019;156(4):976–986.

33. Shin J, Yu JH, Jin YJ, Lee JW. Incidence and Clinical Features of Hepatitis C Virus-associated Hepatocellular Carcinoma Patients without Liver Cirrhosis in Hepatitis B Virus-endemic Area. J Liver Cancer 2021;21(1):34–44.

34. Lewis S, Roayaie S, Ward SC, Shyknevsky I, Jibara G, Taouli B. Hepatocellular carcinoma in chronic hepatitis C in the absence of advanced fibrosis or cirrhosis. AJR Am J Roentgenol 2013;200(6):W610–W616.

35. Huang CF, Awad MH, Gal-Tanamy M, Yu ML. Unmet needs in the post-direct-acting antivirals era: The risk and molecular mechanisms of hepatocellular carcinoma after hepatitis C virus eradication. Clin Mol Hepatol 2024;30(3):326–344.

36. Banerjee A, Ray RB, Ray R. Oncogenic potential of hepatitis C virus proteins. Viruses 2010;2(9):2108–2133.

37. Ludwig DR, Fraum TJ, Cannella R, et al. Expanding the Liver Imaging Reporting and Data System (LI-RADS) v2018 diagnostic population: performance and reliability of LI-RADS for distinguishing hepatocellular carcinoma (HCC) from non-HCC primary liver carcinoma in patients who do not meet strict LI-RADS high-risk criteria. HPB (Oxford) 2019;21(12): 1697–1706.

38. Moctezuma-Velázquez C, Lewis S, Lee K, et al. Non-invasive imaging criteria for the diagnosis of hepatocellular carcinoma in non-cirrhotic patients with chronic hepatitis B. JHEP Rep 2021;3(6):100364.